

Size Effect on Plastic Deformation Capacity of Reinforced Concrete Beams under Shear and Flexure

Sachio KOIKE and Shigemitsu HATANAKA*

曲げとせん断を受ける鉄筋コンクリート梁の

塑性変形性能における寸法効果

小池狭千朗・畑中重光*

A series of bending tests of reinforced concrete (RC) beams of various sizes and uniaxial compression tests of confined concretes used in the compressive zones of the RC beams were carried out to examine their plastic deformational behavior. Based on the test results, the effect of the size of specimens on the deformation behavior of RC beams and confined concretes were discussed. It was found that both the stress-strain behavior of confined concrete and the moment-curvature behavior of RC beams become more brittle with increasing size of specimen regardless of the spacing of stirrups.

1. INTRODUCTION

For the application of plastic design method to reinforced concrete (RC) frames, it is the first requisite that constitutive RC members are ductile enough for the redistribution of moment and for the formation of plastic collapse mechanism. To discuss analytically the deformational capacity of RC members, the effects of various parameters should be fully examined with respect to the characteristics of a plastic hinge of RC members.

The authors have already examined the curvature distribution characteristics of RC beams and found that the increase in ductility in the failure zone of an RC member also accelerates the extension of the failure zone, and as a result, the plastic deformational capacity of the

whole RC member increases [1,2]. The size of specimens tested was, however, much smaller (section of RC beam: 9.7x19.4 cm) than the size of actual RC beams.

The purpose of the present study is to examine the effect of the specimen size on the plastic deformational capacity of RC beams under flexure and shear, and on the ductility of confined concretes under compression.

2. EXPERIMENTAL PROCEDURES

2.1 Outline of experiment

The following two series of experiments were carried out.

(1) RC beams

Outline of the experiment of RC beams is shown in Table 1. Testing variables include the size of a specimen ($b \times h \times$

ls; b:width of specimen, h: depth of specimen, ls: length of shear span of specimen), spacing of stirrups(S), and tensile reinforcement ratio(Pt). Diameters of stirrups were selected for the lateral reinforcement ratio to be approximately 0.3 % for the specimen with stirrups of S=b. The number of beam specimens was 18 for Pt=1.4%, 39 for Pt=2.1%, and 18 for Pt=2.8%; that is , the total number was 75.

Figure 1 shows examples of the detailing of reinforcement of RC beams. Additional longitudinal and web reinforcing bars (web reinforcement ratio was larger than 1.2%) were arranged in one side of the beams, as shown in the figure. Hereinafter, the right hand side of the beams in Fig.1 is referred to as "tested span" and the other side "non-tested span".

Table 1 Outline of experiment of RC beam

Size of beam (h=2b)				S	Pt (%)
Section b×h (cm)	※1 Re. bar	※2 Stirrup (mm)	ℓ _s		
7.3×14.6	D10	φ3.2	4h	b/4	1.4
9.7×19.4	D13	φ3.9	6h	b/2	2.1
12.5×25.0	D16	φ4.9	8h	b	2.8
15.0×30.0	D19	φ5.7			
20.0×40.0	D25	φ8.0			

[Note] ※1: Diameter of longitudinal reinforcing bar
 ※2: Diameter of stirrup, ℓ_s: Length of shear span
 S: Spacing of Stirrup, Pt: Percentage of longitudinal reinforcing bar
 b: Width of beam, h: Height of beam

(2)Concrete prisms

Outline of the experiment of concrete prisms is shown in Table 2. The width(b) of the section of prisms and the arrangement of lateral reinforcement was designed to be consistent with the compressive zones of RC beams. The height(H) of prisms was chosen to be three times the width(b) of the section. The number of specimens prepared for each factor was 12, and the total number was 240.

2.2 Fabrication and curing of specimens

Ordinary Portland cement, river sand (<5 mm), and river gravel (5~25 mm) were used for the fabrication of concrete. Water-cement ratio of 55% was chosen, and slump was 15 cm. The mechanical properties

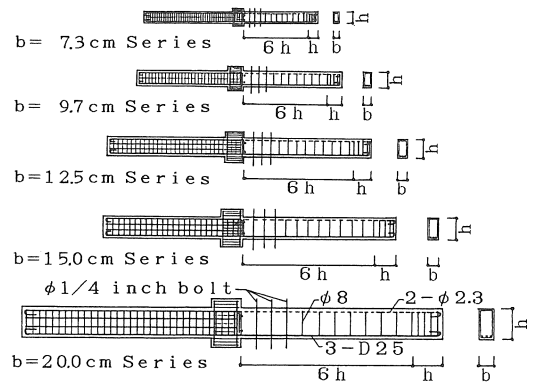


Fig.1 Detailing of reinforcement (ls=6h)

Table 2 Outline of experiment of concrete prism

Size of prism		Hoop	
Section b×b (cm)	Height H=3b (cm)	Diameter φ (mm)	Spacing S
7.3×7.3	21.9	3.2	b/4
9.7×9.7	29.1	3.9	b/2
12.5×12.5	37.5	4.9	b
15.0×15.0	45.0	5.7	∞
20.0×20.0	60.0	8.0	

Table 3 Mechanical properties of longitudinal bar

Diameter (mm)	Yield strength (kgf/cm ²)	Maximum strength (kgf/cm ²)	Elongation (%)
D10	3912	5589	26.5
D13	3644	5325	27.3
D16	3662	5387	24.1
D19	3822	5793	24.1
D25	3640	5714	24.8

of longitudinal and lateral reinforcing bars used are shown in Table 3 and Table 4, respectively. Concrete was cast horizontally for all the specimens, and cured in a room until the tests. Tests were carried out at the age of 6 weeks.

2.3 Methods of loading and measurement

(1) RC beams

The methods of loading and measurements of curvature and deflection

of specimens are illustrated in Fig.2. Concentrated load was applied at the mid-span of the beams whose shear span lengths, i.e. distance from the side face of a column to a supported point, are $4h \sim 8h$ (where, h :depth of beams).

The curvatures and deflections in 1.5h region from the critical section of the tested span were measured by six couples of deformation transducers(D.T.) which were set to the screw bolts embedded in a beam at the pitch of $0.5h$ and at the

Table 4 Mechanical properties of lateral bar

Diameter (mm)	Yield strength (kgf/cm ²)	Maximum strength (kgf/cm ²)	Elongation (%)
3.2	2415	3426	29.2
3.9	2280	3347	40.9
4.9	1937	3069	41.6
5.7	2983	3890	31.5
8.0	2654	3531	32.5

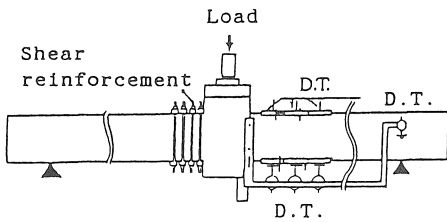


Fig.2 Methods of loading and measurements

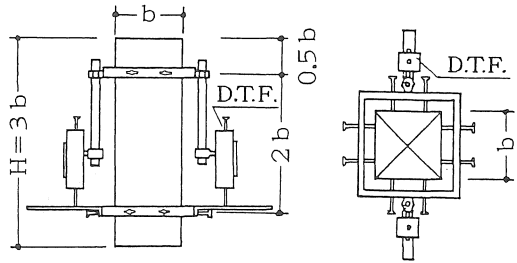


Fig.3 Method of strain measurement

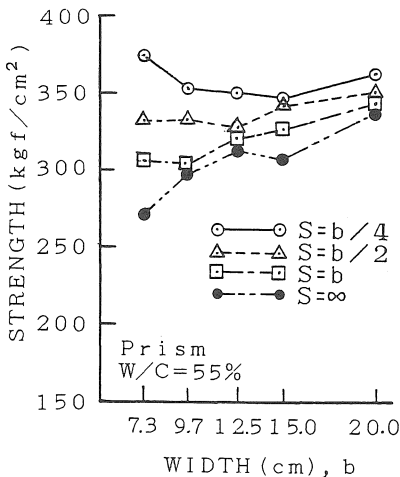


Fig.4 Size effect on compressive strength

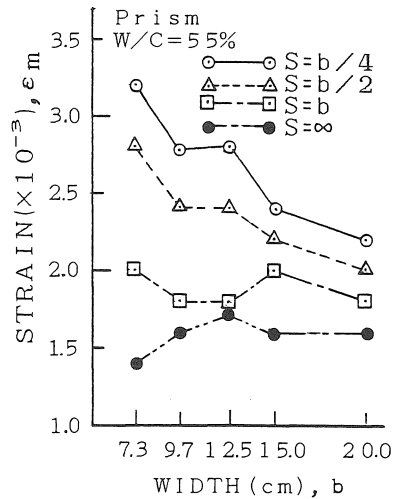


Fig.5 Size effect on strain at peak stress

same level as the top and the bottom surfaces of the beam. Hereinafter, the curvature measured regions are referred to as the "first, second, and third regions" from the critical section. Relative deflection between the critical section and the supported point of the tested span was also measured.

(2) Concrete prisms

The method of strain measurement of concrete prisms is illustrated in Fig.3. Specimens were loaded under the constant

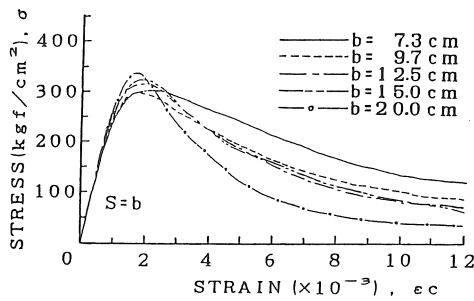
strain rate of about $2 \times 10^{-3}/\text{min.}$ up to the specified strain ($\epsilon = 5 \times 10^{-3}$) in general. The longitudinal strain was measured by a couple of deformation transducers (measurement length was $2b$).

3. TEST RESULTS AND DISCUSSIONS

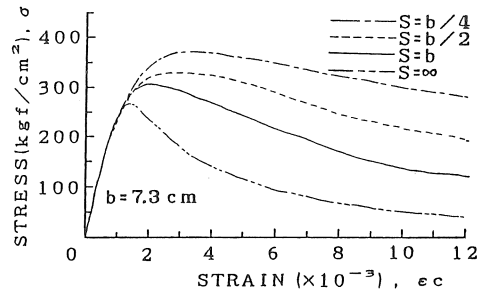
3.1 Concrete prisms

(1) Compressive strength

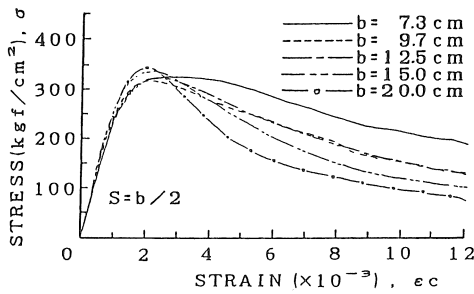
Figure 4 shows the effect of specimen size on the compressive strength of



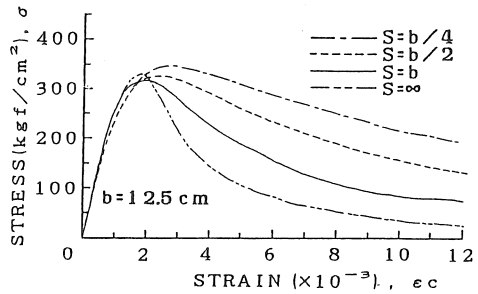
(a) S=b



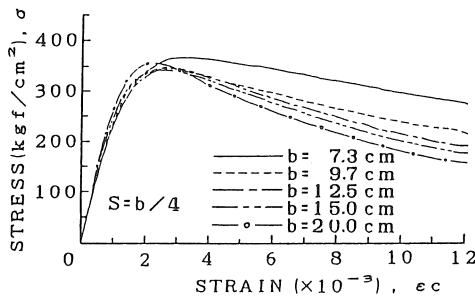
(a) b=7.3 cm



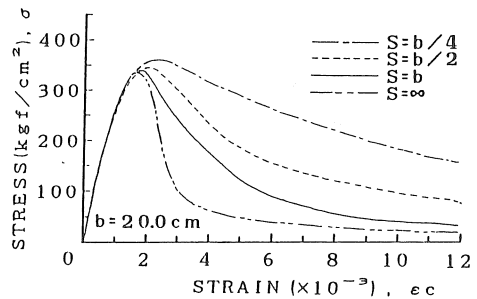
(b) S=b/2



(b) b=12.5 cm



(c) S=b/4



(c) b=20.0 cm

Fig.6 Size effect on stress-strain curve

Fig.7 Effect of spacing of hoops on stress-strain curve

confined concrete for various spacing (S) of hoops. It is shown, for plain concrete ($S=\infty$) and confined concrete with hoops of large spacing ($S=b$), that the compressive strength increases with increasing size of specimen which is similar tendency to the earlier test result of plain concrete [3]. Such size effect, however, is not recognized for confined concrete with hoops of small spacing ($S=b/4, b/2$).

(2) Strain at peak stress

Figure 5 shows the effect of specimen size on the strain (ϵ_m) at the peak stress of confined concrete for various spacing of hoops. It is shown, for plain concrete ($S=\infty$) and confined concrete with hoops of large spacing ($S=b$), that the value of ϵ_m is hardly affected by the specimen size in $b \geq 9.7$ cm. For confined concrete with hoops of small spacing ($S=b/4, b/2$), however, the value of ϵ_m decreases almost constantly with increasing size of specimen.

(3) Stress-strain curve

Figures 6(a) through 6(c) show the effect of specimen size on the stress(σ)-strain(ϵ) curve of confined concrete for the hoops of various spacings. Here, damage of concrete occurred around the mid-height of specimens, so that all the damaged zones were within the strain measurement region of specimens. The figures show that the descending portions of $\sigma - \epsilon$ curves become steeper with

increasing size of specimen regardless of the spacing of hoops.

Figures 7(a) through 7(c) show the effect of spacing of hoops on the $\sigma - \epsilon$ curve of confined concrete for various sizes of specimen. The compressive strength is higher and the descending portion of $\sigma - \epsilon$ curve is less steep for the smaller spacing of hoops. Note that this tendency is more remarkable for smaller specimens.

3.2 RC beams

(1) Moment-curvature curve

Figure 8 shows an example of measured moment index (M/bd^2)-curvature index ($\phi \cdot d$) curve (hereinafter, referred to as $M - \phi$ curve). Note that the moment of each region is represented by the maximum moment in the region, and the $M - \phi$ curves of the first and second regions are represented by envelope curves. Following discussions are based on the envelope curves. The failure pattern of the specimen is illustrated together with the curves.

It is observed in Fig.8 that the measured $M - \phi$ curves of different regions are significantly different from each other. The curvature in the second region does not decrease but increases with the decrease in the moment in the first region. In the third region, curvature decreases with decreasing moment after a

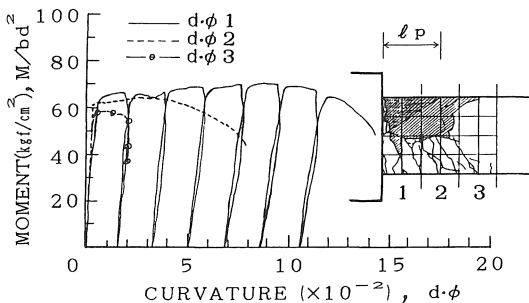


Fig.8 M- ϕ curve of each region

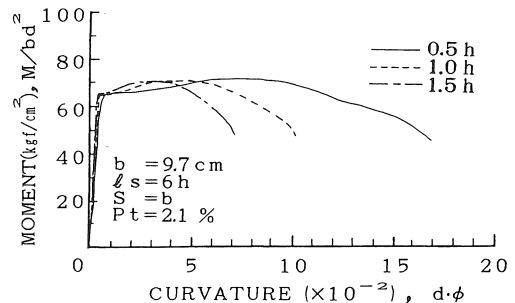
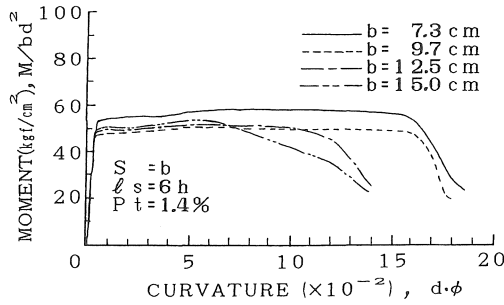


Fig.9 Averaged M- ϕ curve

small amount of plastic curvature developed. Namely, in the first and second regions, plastic deformation starts to develop before the maximum moment of the region reaches the yielding moment in the first region.

Because of the damage localization, measured M- ϕ curves become quite

different depending on the curvature measurement length even in the same specimen. Figure 9 shows the M- ϕ curves averaged over the length of 0.5h, 1.0h, and 1.5h from the critical section. The M- ϕ curve shows more brittle behavior as the curvature measurement length becomes longer.



(a) $Pt = 1.4\%$

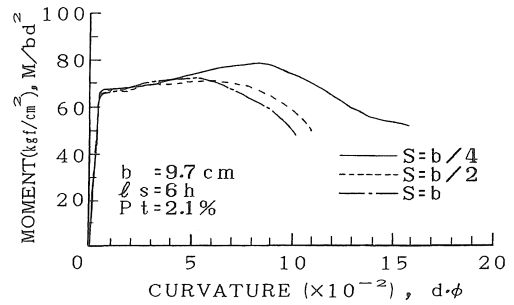
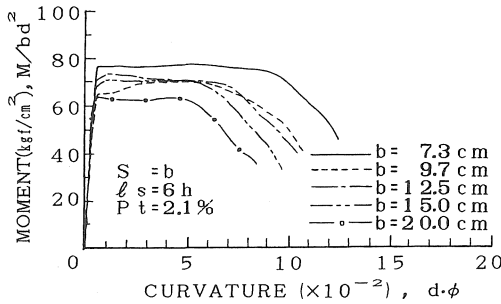
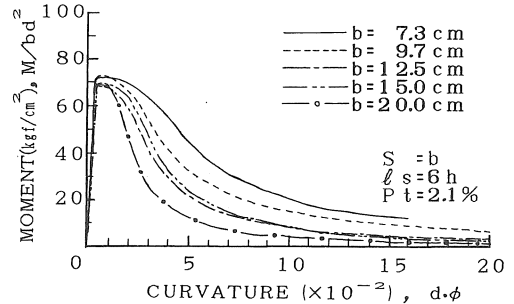


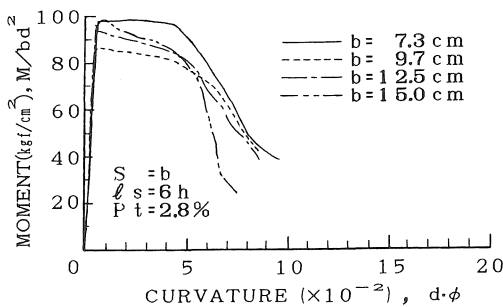
Fig.11 Effect of stirrup spacing on M- ϕ curve (1.0h region)



(b) $Pt = 2.1\%$

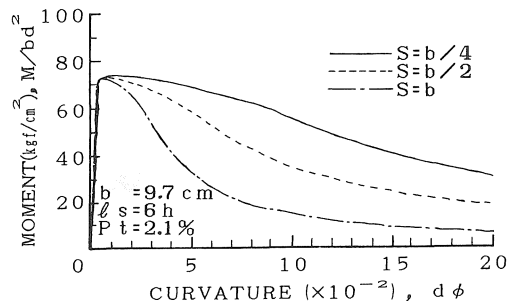


(a) Effect of specimen size (b)



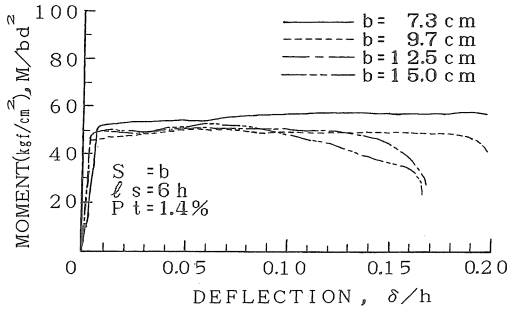
(c) $Pt = 2.8\%$

Fig.10 Size effect on M- ϕ curve (1.0h region)

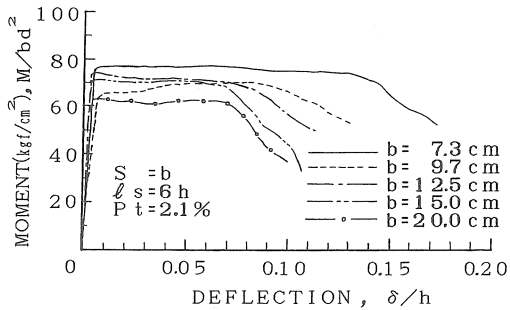


(b) Effect of spacing (S) of hoops

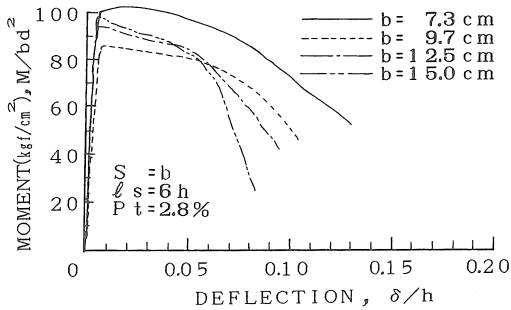
Fig.12 Calculated M- ϕ curve



(a) Pt=1.4%



(b) Pt=2.1%



(c) Pt=2.8%

Fig.13 Size effect on M- ϕ curve (1.5h region)

The damage generally concentrated in the 1.0h region from the critical section. Therefore, based on the averaged M- ϕ curves of the first and second regions, the effects of various factors on the flexural deformational capacity of RC beams are discussed in the following. Figures 10(a) through 10(c) show the size effect in the M- ϕ curves of the specimens

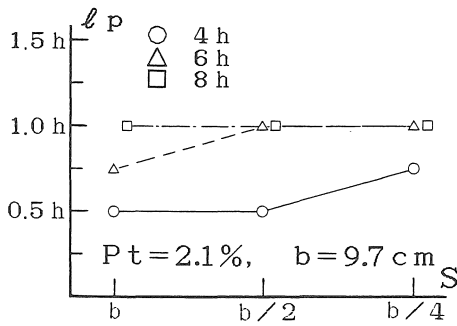
of $l_s=6h$, $S=b$ for various values of P_t . The M- ϕ curves of smaller size specimen is in general more ductile, which is consistent with the tendency of the $\sigma - \epsilon$ curves of concrete specimens. Figure 11 shows the effect of stirrup spacing on M- ϕ curves. The smaller the spacing of stirrups, the more ductile becomes the M- ϕ curve.

Figures 12(a) and 12(b) show the M- ϕ curves obtained by the calculation with the $\sigma - \epsilon$ curves of concrete prisms and steel bars. The analytical curves represent qualitatively similar tendency concerning the effects of the specimen size and stirrup spacing to the experimental curves in Figs.10(b) and 11. However, all the analytical curves show more brittle behavior than the experimental ones to be compared.

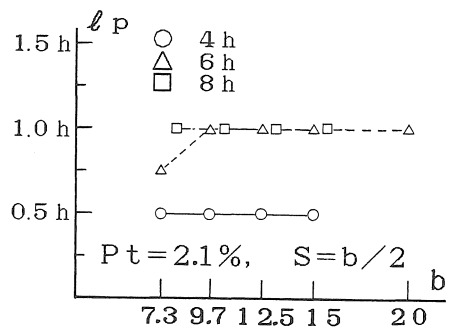
(2) Deflection of 1.5h region

As is mentioned in Section 3.2(1), the damage generally concentrated in the 1.0h region from the critical section. Therefore, it is considered possible to predict the deformational capacity of a whole beam by evaluating the relative deflection of 1.5h region from the critical section including the elastic zone free from outstanding damage. Note that, although the shear deflection may be negligible as far as the ultimate deflection of the whole beam is concerned, the contribution of shear deflection to the total deflection is not so small compared with flexural deflection in such a short length of 1.5h [4].

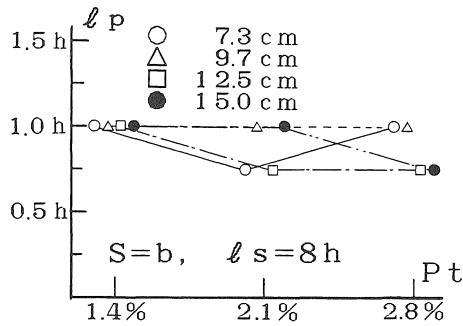
Figures 13(a) and 13(b) show the size effect in the deflection (δ) of the 1.5h region of the specimens of $S=b$, $l_s=6h$. Here, the deflection (δ) is normalized by the height (h) of a beam in the x-axis to discuss the size effect. It is seen in the figure that $M/bd^2 - \delta/h$ curves (M- δ curve) of smaller size specimens are in general more ductile, which is consistent with the tendency of the M- ϕ curves of 1.0h region. Further, the same tendency is observed in the beams of $l_s=4h$ and $8h$.



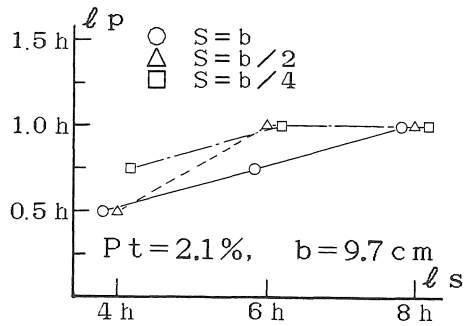
(a) Spacing of stirrups (S)



(b) Size of specimen (b)



(c) Tensile reinforcement ratio (Pt)



(d) Shear span length (ls)

Fig.14 Effect of each factor on l_p

(3) Length of failure zone

To evaluate quantitatively the effect of various factors on the $M-\phi$ relations of RC beams, the tested spans of RC beams were idealized into two zones, i.e. failure and non-failure zones, according to the degree of damage [1,2]. Figures 14(a) through 14(d) show the effect of each factor on the length of idealized failure zone (l_p). Here, regions where the compressive fiber strain exceeded 0.004 were regarded as the failure zone [1].

According to the figures, i) the value of l_p tends to increase with the decrease in the spacing (S) of stirrups (Fig.14(a)), ii) it is hardly affected by the specimen size (b) and tensile reinforcement

ratio (Pt) (Figs.14(b) and 14(c)), and iii) the value of l_p increases with the increasing length (l_s) of shear span (Fig.14(d)). In addition to the statement of iii), note that the behavior of a section within the failure zone (l_p) is also greatly affected by the shear span length, i.e., the behavior becomes more ductile with decreasing shear span length due to the effect of moment gradient [2].

4. CONCLUSIONS

The following conclusions can be drawn from the present study.

- 1) Both the stress-strain curve of confined concrete prisms and moment-curvature curve of RC beams become more brittle with increasing size of specimen regardless of the spacing of stirrups.

2) The size effect on the length of failure zone (l_p) was hardly observed. Therefore, the size effect on the Moment-curvature curve is considered greatly due to the size effect on the stress-strain behavior of concrete in the compressive zone of a beam. The effect of the other factors on l_p was found almost the same as in the previous report [2].

REFERENCES

1) Hatanaka, S., Kosaka, Y., Tanigawa, Y. and Miwa, R., "Curvature Localization in Plastic Deformation Range of RC Beams Under Flexure," Jour. of Struct. and Const. Eng. (Trans. of AIJ), No. 371, Jan. 1987, pp. 27-38.

2) Kosaka, Y., Tanigawa, Y., Hatanaka, S. and Miwa, R., "Plastic Hinge of Reinforced Concrete Beams," Trans. of Cem. Assoc. of Japan, Vol. 40, 1986, pp. 580-583 (in Japanese).

3) Koike, S., Okufuji, K. and Okuya, Y., "Size Effect on Expression for Stress-Strain Curves of Concrete Under Compression and its Application for Moment-Curvature Relationships of Reinforced Concrete Beams," Trans. of JCI, Vol. 9, 1987, pp. 249-256.

4) Hatanaka, S., Kosaka, Y. and Tanigawa, Y., "Modeling of Plastic Zone for RC Beams of Flexural Deformation Predominating Type," Proc. of Ninth World Conf. on Earthquake Eng., Tokyo-Kyoto, Japan, Vol. 4, 1988, pp. 457-462.

(受理 平成2年3月20日)